CRISPR MEDIATED *RAB3D* KNOCKOUT PROMOTES MELANOMAGENESIS IN PLATYFISH

by

Angel Orlando Sandoval

HONORS THESIS

Submitted to Texas State University
in partial fulfillment
of the requirements for
graduation in the Honors College
December 2020

Thesis Supervisor:

Yuan Lu

FAIR USE AND AUTHOR'S PERMISSION STATEMENT

Fair Use

Duplication Permission

ACKNOWLEDGEMENTS

I'd like to thank my mentors at the *Xiphophorus* Genetic Stock Center who include but are not limited to Yuan Lu, Raquel Salinas, Ronald B. Walter, William Boswell, Mikki Boswell, Markita Savage, and Cristina Mendoza whose expertise were invaluable in formulating, executing, and analyzing my research ideas. Their grand support and expertise brought my work to a high level. Through everyone's aid, I was able to develop myself and grow as a scientist. This research was a team effort, and it would not have been possible without any of my colleagues. Lastly, thank you to Rosa Vasquez, Oscar Sandoval, and Osvaldo Sandoval for their encouragement, insight, and inquisitiveness.

- If everything were perfect, perfect would be dull.

TABLE OF CONTENTS

Page

LIST OF TABLES

Table **Page**

LIST OF FIGURES

Figure **Page**

LIST OF ABBREVIATIONS

- BC: Backcross generation
- EDTA: Ethylenediaminetetraacetic acid
- *EGFR/egfr*: Epidermal Growth Factor Receptor
- gDNA: genomic DNA
- GKA: Gordon-Kosswig-Anders
- nt: Nucleotide
- PCR: Polymerase Chain Reaction
- *Rab3d*: Ras-related protein Rab-3D
- Sd: Spotted dorsal
- Sg: Single-guide
- TAE: Tris-acetate-ethylenediaminetetraacetic acid
- *X. hellerii*: *Xiphophorus hellerii*
- *X. maculatus*: *Xiphophorus maculatus*
- *xmrk: Xiphophorus* Melanoma Receptor Kinase

ABSTRACT

Xiphophorus interspecies hybrids, i.e., *X. hellerii* × (*X. maculatus* Jp 163 A × *X. hellerii*) display melanomagenesis according to Mendelian segregation of an oncogene, *xmrk*, and a recently identified melanoma regulator, *rab3d*. The *rab3d* gene's function in the *Xiphophorus* genome is hypothesized to inhibit the driving oncogene *xmrk*. It is thought that by including both an oncogene and tumor suppressor within its genome, *Xiphophorus* protect themselves from genome incompatibilities that may arise as a result of interspecies hybridization as explained by the Bateson–Dobzhansky–Muller model. Genotype and transcriptional analyses elucidated *rab3d* to serve as the gene responsible for *Xiphophorus'* inherited tumor regulator. Functional analyses of *rab3d* in *Xiphophorus* have yet to be performed. Therefore, to investigate mechanism of the *xmrk-rab3d* molecular interaction that represses tumorigenesis, we report *in vitro* CRISPR mediated knockout of *rab3d* in *Xiphophorus* Jp163 A. Our findings provide insight into melanoma etiology and further our molecular understanding of the *xmrk-rab3d* interaction.

I. Introduction

The Gordon-Kosswig-Anders (GKA) animal model, derived from the *Xiphophorus* system, serves as a translational model to study the etiology of melanoma and cancer genetics. Maintained since the 1920's, the *Xiphophorus* system is one of the oldest and was the first animal model to provide evidence that melanoma is induced by negative epistasis [1-3]. This allows for the utilization of highly inbred lines of animals that have similar genomic profiles. Furthermore, *Xiphophorus* comprising the GKA model present the unique ability to produce fertile inter-species hybrids [1-3]. The *X. maculatus* genome encodes two genes that have been linked to melanoma: Ras-related protein Rab-3D (*rab3d*) and a mutant duplicate of Epidermal Growth Factor Receptor (*egfr*) termed *Xiphophorus* Melanoma Regulatory Kinase (*xmrk*) [4,5]. The *xmrk* gene serves as an oncogene, and *X. maculatus' rab3d* serves as a tumor suppressing gene by *r*egulating *d*ifferentiation (R(Diff)) [4]. Due to its inbred nature, *X. maculatus* are homozygous for both *rab3d* and *xmrk*. The two genes within *X. maculatus* present phenotypically as a nevus-like pigmentation pattern on its dorsal fin; herein referred to as *spotted dorsal* (*Sd*). When *X. maculatus* is mated with *Xiphophorus hellerii* (*X. hellerii*), the resulting F_1 hybrids, containing single *X.* maculatus-derived *rab3d* and *xmrk* alleles, display an enhanced dorsal fin pigmentation pattern due to the inheritance of one tumor suppressing gene, *R(Diff)*, and one copy of the oncogene, *xmrk*. The backcross progeny, resulting from mating F_1 with *X. hellerii*, present with three phenotypes following Mendelian segregation: 25% of the backcross progeny present with lethal exophytic melanoma due to the absence of *R(Diff)* and presence of *xmrk*, 25% present with enhanced *Sd* (identical phenotype and genotype to F_1), and 50% present with no phenotypic abnormalities due to

the absence of both *xmrk* and *R(Diff)* [2,6,7]. The difference between the *rab3d* alleles between *X. maculatus* and *X. hellerii* is a single amino acid change from an asparagine residue in *X. maculatus* to a lysine residue in *X. hellerii* (N204K, *X. maculatus* to *X. hellerii*).

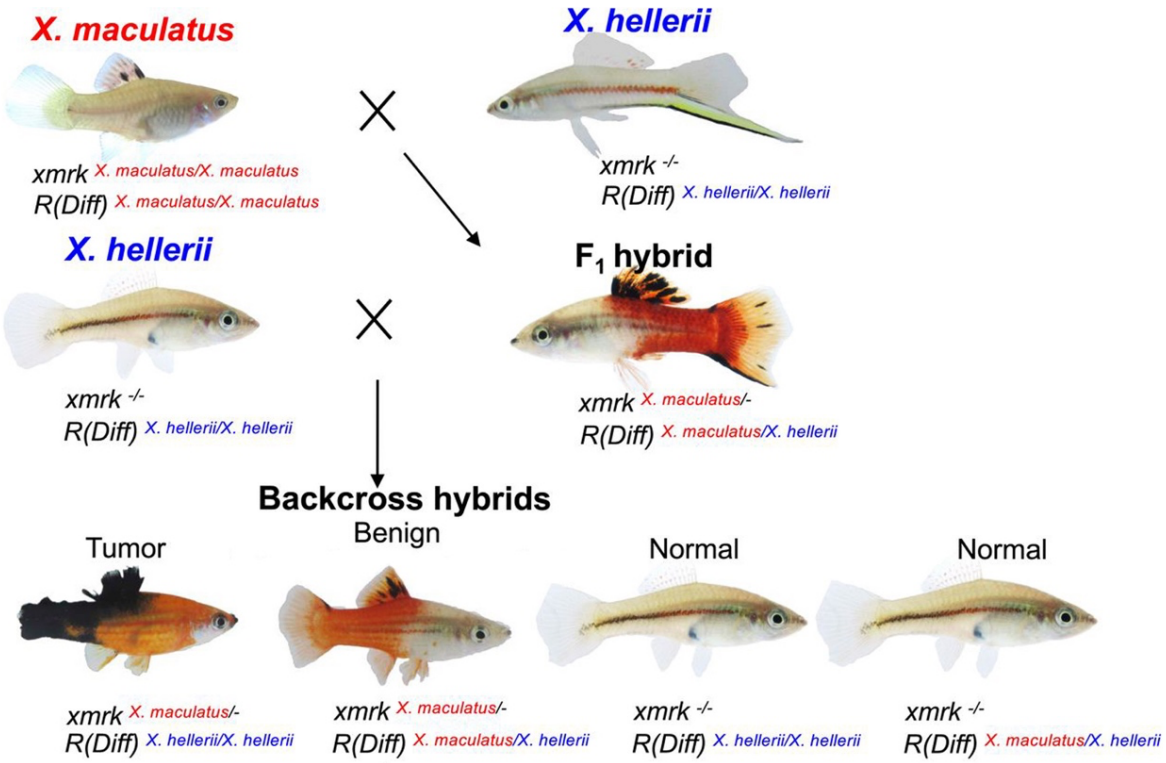

Fig. 1: GKA Animal Model. The crossing scheme shows the *Xiphophorus* species used to produce F_1 and BC_1 interspecies hybrids. *X. maculatus* Jp163 A and *X. hellerii* are used to produce F_1 hybrids artificially. The F_1 hybrids are subsequently backcrossed to *X. hellerii* to produce BC_1 hybrid progeny [8].

Melanocytes are responsible for providing their melanin pigmentation to local keratinocytes. This process gives keratinocytes the ability to shield against ultraviolet radiation-induced DNA damage in dermal regions [9-11]. Melanoma results from the development of malignant melanocytes. This leads to the melanotic presentation of melanoma [12].

The incidence of melanoma has risen over the past four decades [13]. In fact,

approximately 300,000 global cases are currently diagnosed annually [14-16]. Current treatments such as surgical excision and chemotherapy remain standard in healthcare [14,17]. Immunotherapeutics such as vemurafenib for $BRAF^{V600E}$, ipilimumab for increased T-cell activity, and nivolumab and pembrolizumab for continuation of an immune response have recently advanced treatment of melanoma [18-22]. However, these treatment methods have not proven favorable, as common therapeutics and surgical resection techniques have resulted in poor prognosis [17,23]. Additionally, drug toxicity, limited therapeutic options, and emerging resistance further dampen the practicality of treatment by the aforementioned means [24,25]. *BRAF* and *NRAS* mutations are present in approximately 50 % and 28 % of melanomas, respectively. Additionally, only 48 % of patients dosed with Vemurafenib for *BRAF* mutant melanoma and 15 % dosed with Binimetinib for *NRAS* mutant melanoma display an overall response to therapy which leaves a majority of these melanoma patients without treatment options [19,26]. Thus, there is a prevalent need for further research into alternative therapeutics against melanoma.

Advances in molecular genetics have led to the potential to treat melanoma through the use of genetic targets. One such molecular system is the Clustered Regularly Interspaced Short Palindromic Repeats (CRISPR) system in which RNA guides are used to direct the CRISPR associated protein (Cas) nuclease to a specific locus where a double strand break is induced. This double strand break, along with the cell's inherent DNA repair mechanisms, can be used to knock out oncogenes, knock in tumor-suppressing genes, transcriptionally activate tumor suppressing genes, introduce modified T-cells, or introduce suicide genes; all of which can be used to treat melanoma [27-35]. Thus, a highly accurate and efficient CRISPR-Cas system may be revolutionary in the clinical battle

against melanoma. Recent studies provide promising results for genetic modification in the treatment of melanoma [35-37].

The association of the *rab3d* gene with cancer lends itself to being a proper CRISPR target for knockout studies. Rab GTPases serve as intracellular transport proteins responsible for exocytic trafficking [38]. With regard to cancer etiology, *rab3a* is involved with glioma initiation, *rab3b* is transcriptionally upregulated in prostate cancer patients contributing to tumor cell survival, and *rab3c* has been shown to be upregulated in colon cancer patients [39-42]. *rab3d*'s function is derived from both its transcriptional levels and pre- and post-translational modifications [8,43]. For example, high transcriptional levels of *rab3d* are associated with a multitude of cancers [40]. Clinically, up-regulation of *rab3d* is associated with poor prognosis within patients presenting with colorectal cancer [44]. In the rat pancreatic acinar cell line AR42J, carboxyl-methylation is noted, potentially signifying a relation between carboxyl-methylation of *rab3d* and cancerous development [43]. Considering prior studies, it is hypothesized that *rab3d* activity is detrimental since its expression is correlated with disease presentation. However, we hypothesize that *rab3d* withholds a tumor suppressing function, and its upregulation in disease is a side effect of defense against awry processes such as cancer. We hypothesize that a *rab3d* knockout in an animal known to contain a natural oncogenic driver for melanoma, such as *X. maculatus,* will lead to melanotic presentation. To our knowledge, no such *rab3d* knockout studies have been performed upon vertebrates who have the potential to naturally develop melanoma thus far.

To begin to study the effects of *rab3d* knockouts *in-vivo*, we excised *rab3d* exon 1 *in vitro* using CRISPR-Cas9 to target *rab3d*. Herein, we present *rab3d* knockouts in *X.*

maculatus JP 163 A animals *in vitro*.

II. MATERIALS AND METHODS

Xiphophorus Animal Model:

X. maculatus Jp163 A, *X. hellerii* (Rio Sarabia), and first generation backcross (BC_1) animals used in this study were provided by the *Xiphophorus* Genetic Stock Center, San Marcos, Texas (https://www.xiphophorus.txstate.edu). *X. maculatus* Jp 163 A females were artificially inseminated with sperm from male *X. hellerii* to produce F_1 progeny. F_1 hybrid males were backcrossed to *X. hellerii* females to generate the BC_1 animals. Fish were sacrificed by placement into an ice bath until gill movement was suspended. Cranial resection was then performed. Organs were dissected and stored in RNAlater (Ambion Inc.). Organs in RNAlater were stored at -20 °C for 24 hr. After 24 hr, the RNAlater solution was aspirated out, and the dry organs were stored at -80 °C indefinitely or until use. Fish were maintained and utilized in accordance with protocols approved by Texas State University IACUC (IACUC7381).

Design of CRISPR-Cas Targets:

CRISPR-Cas guide RNA's were created within the *rab3d* exon 1 in the *X. maculatus* Jp163 A genome. Single-guide (sg) RNA's were designed using CCTop's CRISPR/Cas9 target online predictor at COS Heidelberg (https://crispr.cos.uni-heidelberg.de/); the online tool was built by fish genome specialists in Dr. Jochen Wittbrodt's lab.

In vitro synthesis of sgRNA:

sgRNAs were designed using CCTop, and were produced using Guide-it™ sgRNA In Vitro Transcription and Screening System (Takara Bio). A 56-nucleotide (nt) to 58-nt forward primer was designed for each cut site. sgRNA primers designed

targeting *rab3d*'s exon 1 can be found in Table 1 and viewed schematically in Fig. 2. The sgRNA's were produced following manufacture's protocol.

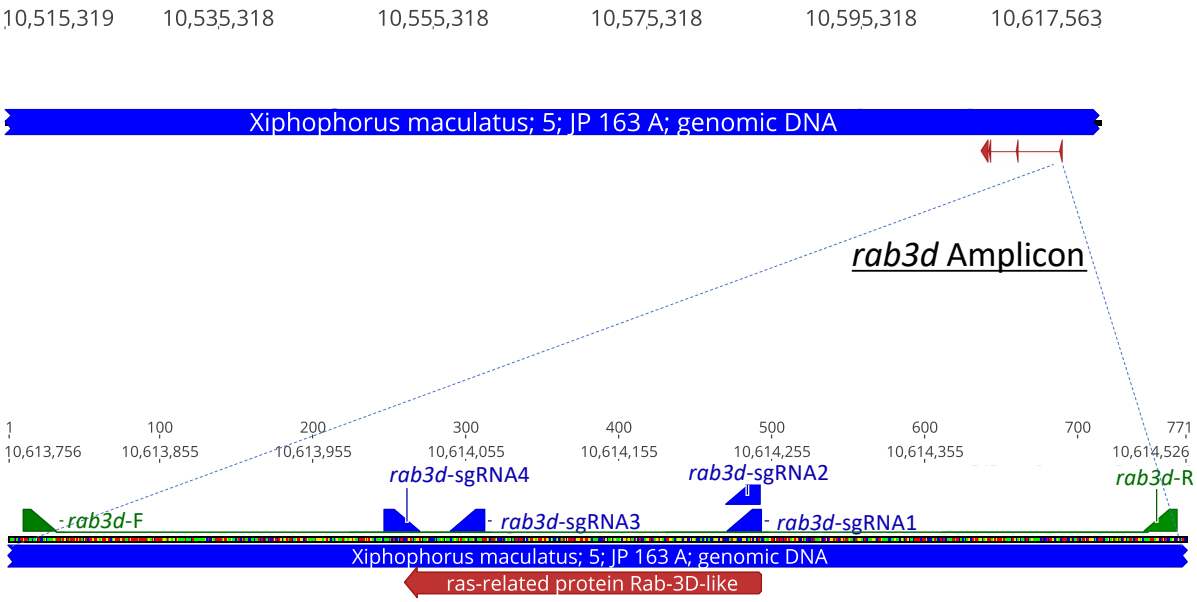

Fig. 2: sgRNA Targets: The top blue ribbon represents *X. maculatus* JP 163 A genomic DNA from chromosome 5 (10,515,319 – 10,617,563) nt. The bottom blue ribbon represents a zoomed in depiction of the genomic region of *rab3d* exon1. The green markers indicate the locations of *rab3d* forward and reverse primers. The blue markers above the ribbon represent the locations of *rab3d*-sgRNA(1-4) along the genome. The red arrow indicates the location of *X. maculatus' rab3d* 3' end.

Table 1: sgRNA Primers for sgRNA *in vitro* transcription.

Name	Sequences (5'-3')
rab3d-sgRNA1	CCTCTAATACGACTCACTATAGGATGGCGCTAGCCCGGGACCTGTTTAAGAGCTATGC
rab3d-sgRNA2	CCTCTAATACGACTCACTATAGGTGGCGCTAGCCCGGGACCTAGTTTAAGAGCTATGC
rab3d-sgRNA3	CCTCTAATACGACTCACTATAGGTTAAAGTCAAGACAATCTACGTTTAAGAGCTATGC
rab3d-sgRNA4	CCTCTAATACGACTCACTATAGGTTTATCACCTCACCCAGATCGTTTAAGAGCTATGC

Design of Primers Surrounding CRISPR-Cas Cut Sites:

Primers were created using NCBI's BLAST tool [45]. Primers were chosen to amplify sites containing the previously identified sgRNA binding sites. The sequences of

the primers designed for PCR amplification by NCBI's BLAST tool can be found in Table 2 and viewed schematically in Fig. 2.

Table 2: Primers for PCR Amplification.

Name	Sequences (5'-3')	DNA Template Source	Amplicon Length (bp)
rab3d-F	CAACCGCTAAAGCACATCTG	*X. maculatus* Jp163 A	754
rab3d-R	GTTGGGGCTTTCCTTTCCAG		

DNA Isolation:

DNA was isolated using Qiagen DNeasy Blood & Tissue Kit following manufacturer protocol. DNA was then quantified using Qubit 2.0 following manufacturer protocol (Life Technologies, Grand Island, NY, USA).

Polymerase Chain Reaction and Sequencing:

Polymerase chain reaction (PCR) was performed upon the isolated genomic DNA (gDNA) using *rab3d* primers. 10X standard *taq* reaction buffer and *taq* DNA polymerase were provided for by New England Biolabs (Cat. No. M0273S). 10 mM dNTP mix was acquired from ThermoFisher (Cat. No. 18427013). The PCR protocol used was 180 s initial denaturation, followed by 32 cycles of 30 s at 95 °C, 30 s at 52 °C, 70 s at 68 °C, and a final elongation of 300 s at 68 °C. Amplicon was then purified using QIAquick PCR Purification Kit following manufacturer protocols. For products with one prominent band and artifacts, QIAquick Gel Extraction Kit was used following manufacturer protocol to remove the artifacts. Once purified, DNA samples were again quantified by Qubit 2.0, prepared for sequencing, and sequenced by GENEWIZ, LLC.

***In vitro* sgRNA CRISPR-Cas9 Screening:**

Guide-it^{TM} sgRNA In Vitro Transcription and Screening System (Takara Bio) was used to screen sgRNA cleavage upon *rab3d* amplicon following manufacturer's protocol.

Gel Imaging:

Gel electrophoresis was performed upon our *rab3d* amplicon to measure the molecular weight of the product. 50x Tris-acetate-ethylenediaminetetraacetic acid [EDTA] (TAE) buffer was prepared by mixing 242 g tris base, 57.1 mL glacial acetic acid, 100 mL 0.5 M EDTA (pH 8.0), and adjusting the volume to 1 L. 1 x TAE was then prepared and used as both running and loading buffers. A 2% agarose gel was stained with ethidium bromide and prepared using UltraPure™ Agarose by Inivtrogen (Cat. No. 15510-027). After the *in vitro* sgRNA CRISPR-Cas9 Screening, the products were loaded onto the 2 % agarose gel and underwent gel electrophoresis. A 50 bp ladder by Invitrogen was run adjacent to products (ThermoFisher Cat. No. 10416014). Gels were imaged using Fotodyne's FOTO/Analyst FX benchtop darkroom (Fisher Scientific, Cat. No. F71720DLN). The gel imaging software used was FOTO/Analyst PC Image.

Bioanalyzer:

An electronic gel-electrophoresis was performed using Agilent's Bioanalyzer 2100 (Agilent, Cat. No. G2939BA) following manufacturer protocols; Agilent's DNA 1000 Kit was used (Agilent, Cat. No. 5067-1504).

III. Results

Sequence of *rab3d* amplicon

PCR amplicon (*rab3d*) using primers *rab3d*-F and *rab3d*-R was run on a 2% agarose gel and exhibited an amplicon size of 754 nt. This size is consistent with expected amplicon size (Fig. 2,3).

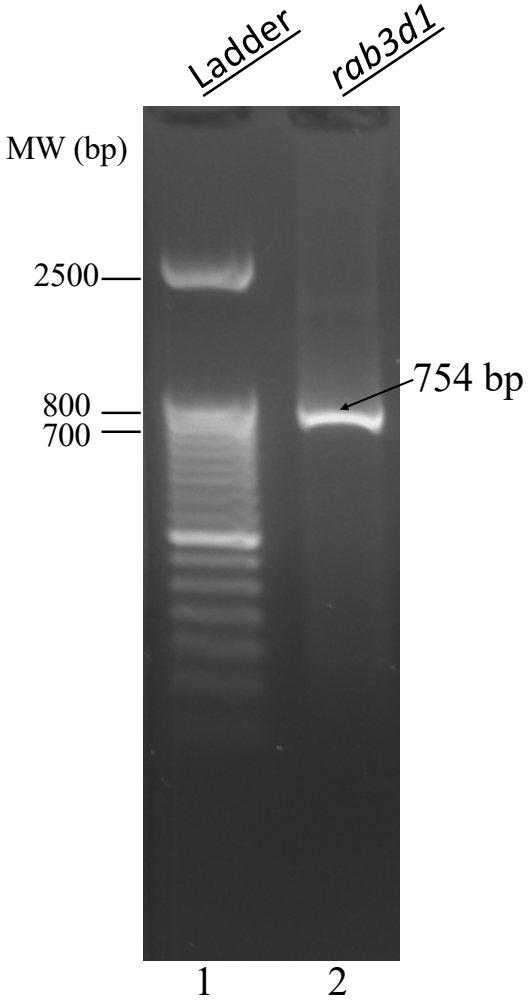

Fig. 3: *rab3d* Amplicon: 1: Ladder, 2: *rab3d* amplicon. Molecular weight labeled to the right is that expected of the *rab3d* amplicon.

The *rab3d* amplicon was subsequently sequenced using Sanger sequencing method. Amplicon sequence was compared to reference genome sequence using Blastn

and displayed 100% match to expected PCR product (Fig. 4).

```
>PREDICTED: Xiphophorus maculatus ras-related protein Rab-3D-like
(LOC102238335), mRNA,
Sequence ID: XM_005809082.3
Range 1: 235 to 471
Identities:237/237(100%),  Gaps:0/237(0%), Strand: Plus/Minus

Query  217  CCCAGATCTGGAGCTTGACCCTCTTGTCGTTCCTGTAGATTGTCTTGACTTTAAAGTCAA  276
            ||||||||||||||||||||||||||||||||||||||||||||||||||||||||||||
Sbjct  471  CCCAGATCTGGAGCTTGACCCTCTTGTCGTTCCTGTAGATTGTCTTGACTTTAAAGTCAA  412

Query  277  TGCCCACTGTGCTCACAAACGCTGAGGTGAAGGAGTCGTCTGCATAGCGAAACAGGAAGG  336
            ||||||||||||||||||||||||||||||||||||||||||||||||||||||||||||
Sbjct  411  TGCCCACTGTGCTCACAAACGCTGAGGTGAAGGAGTCGTCTGCATAGCGAAACAGGAAGG  352

Query  337  AGGTCTTTCCCACGCTGCTGTTGCCGATGATCAGCACCTTGAACATGTAGTCAAAGTTCT  396
            ||||||||||||||||||||||||||||||||||||||||||||||||||||||||||||
Sbjct  351  AGGTCTTTCCCACGCTGCTGTTGCCGATGATCAGCACCTTGAACATGTAGTCAAAGTTCT  292

Query  397  GGTCGGCCGCGTCCCTCTGCTCCTGGCCGACCCCTAGGTCCCGGGCTAGCGCCATCT  453
            |||||||||||||||||||||||||||||||||||||||||||||||||||||||||
Sbjct  291  GGTCGGCCGCGTCCCTCTGCTCCTGGCCGACCCCTAGGTCCCGGGCTAGCGCCATCT  235
```

Fig. 4: Amplified Sequence Identity: The *rab3d* amplicon (Sbjct) displayed 100% matching sequence identity to *rab3d* in the published *X. maculatus* genome (Query).

In vitro Screening of sgRNA

Multiple sgRNA's were created for *in vitro* testing to determine the best candidates for use *in* vivo. It is known that different sgRNA guides provide different cleavage efficiencies, and an sgRNA that works *in silico* might not work *in vivo* or *in vitro* [46-49]. We cleaved *rab3d* exon 1 *in vitro* using sgRNA's 1-4 as guides to determine efficacy and measure the various cleavage efficiencies of each sgRNA should cuts be induced. Expected and acquired fragment sizes after *rab3d* cleavage with sgRNA's 1-4 are concurrent with each other (Table 3). Of interest, sgRNA's 1 and 2 did not result in complete cleavage of our *rab3d* amplicon. sgRNA 4 resulted in almost complete cleavage of our *rab3d* amplicon, and sgRNA 3 led to complete amplicon cleavage (Fig. 5). As this *in vitro* analysis is meant to serve as an *in vivo* indicator of knockout efficiency, it is clear that sgRNA's 3 and 4 would lead to greater knockout efficiencies and hence should be

carried through to *in vivo* analysis. It is known that two double stranded breaks created by the use of dual sgRNA are more effective at creating *in vivo* genomic deletion than are single double stranded breaks induced by single sgRNA. Therefore, we tested the efficiency of *in vitro* cuts using two sgRNA to predict *in vivo* behavior [46]. sgRNA 1 + 4, 2 + 3, 2 + 4, and 3 + 4 proved favorable in creating two *in vitro* cuts upon our *rab3d* amplicon since our acquired fragment sizes matched expected fragment sizes. Through gel analysis, it is clear that sgRNA's 3 and 4 are the best candidates to carry into *in vivo* knockout analyses since these two sgRNA's both 1) display fragment sizes that are easily separable by gel electrophoresis, and 2) display the highest cleavage efficiency of our *rab3d* amplicon (Table 3; Fig. 4, 5).

Table 3: Fragment Sizes. The table lists the *rab3d* amplicon and sgRNA's used to cleave *rab3d* exon 1 under Name. Expected Fragment Size lists the expected fragment sizes after cleavage with the sgRNA's in row. Acquired Fragment Sizes lists quantitative data acquired form bioanalyzer analysis of *in vitro* sgRNA analysis upon our *rab3d* amplicon. The *rab3d* amplicon length is listed under *rab3d* Amplicon Length. All molecular weight measurements are in base pairs (bp). * represents data not acquired through bioanalyzer analysis, but analysis was instead performed by agarose gel electrophoresis.

Name	Expected Fragment Sizes (bp)	Acquired Fragment Sizes (bp)	*rab3d* Amplicon Length (bp)
rab3d	754	*	754
rab3d-sgRNA1	288 + 466	290 + 472 + 768	
rab3d-sgRNA2	289 + 465	290 + 468 + 762	
rab3d-sgRNA3	285 + 469	284 + 469	
rab3d-sgRNA4	253 + 501	254 + 500	
rab3d-sgRNA1 + 4	213 + 253 + 288	758 + 211 + 256 + 291	
rab3d-sgRNA2 + 3	180 + 285 + 289	*	
rab3d-sgRNA2 + 4	212 + 253 + 289	756 + 211 + 257 + 293	
rab3d-sgRNA3 + 4	32 + 253 + 469	26 + 257 + 477	
Control sgRNA + Control Fragment	614 + 350 + 264	631 + 349 + 263	

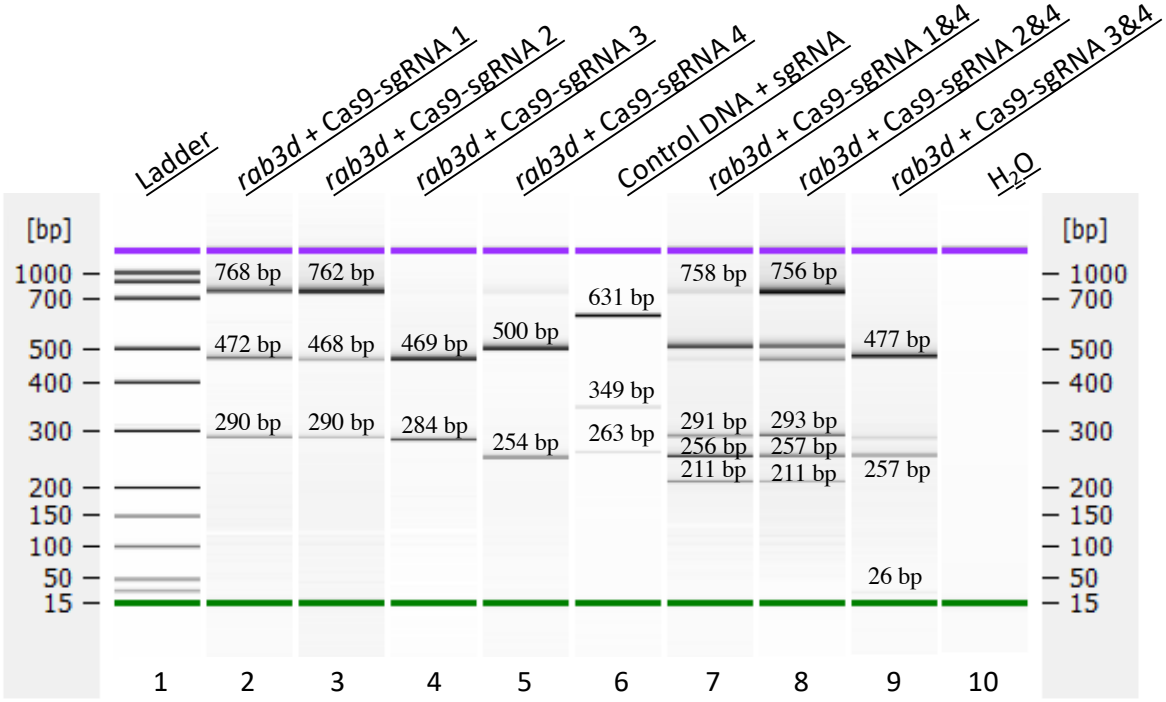

Fig. 5: sgRNA(1-4)-CRISPR-Cas9 *in vitro* Screen upon *rab3d* Amplicon: 1: Ladder, 2: *rab3d* amplicon cut by Cas9-sgRNA 1, 3: *rab3d* amplicon cut by Cas9-sgRNA 2, 4: *rab3d* amplicon cut by sgRNA 3, 5: *rab3d* amplicon cut by sgRNA 4, 6: manufacturer positive control with control Cas9-sgRNA, 7: *rab3d* amplicon cut by Cas9-sgRNA's 1&4, 8: *rab3d* amplicon cut by Cas9-sgRNA's 2&4, 9: *rab3d* amplicon cut by Cas9-sgRNA's 3&4, 10: water (negative control). Molecular weights labeled are those acquired by the bioanalyzer with manufacturer settings. Off target products and those too faint to be quantified by the bioanalyzer are not labeled.

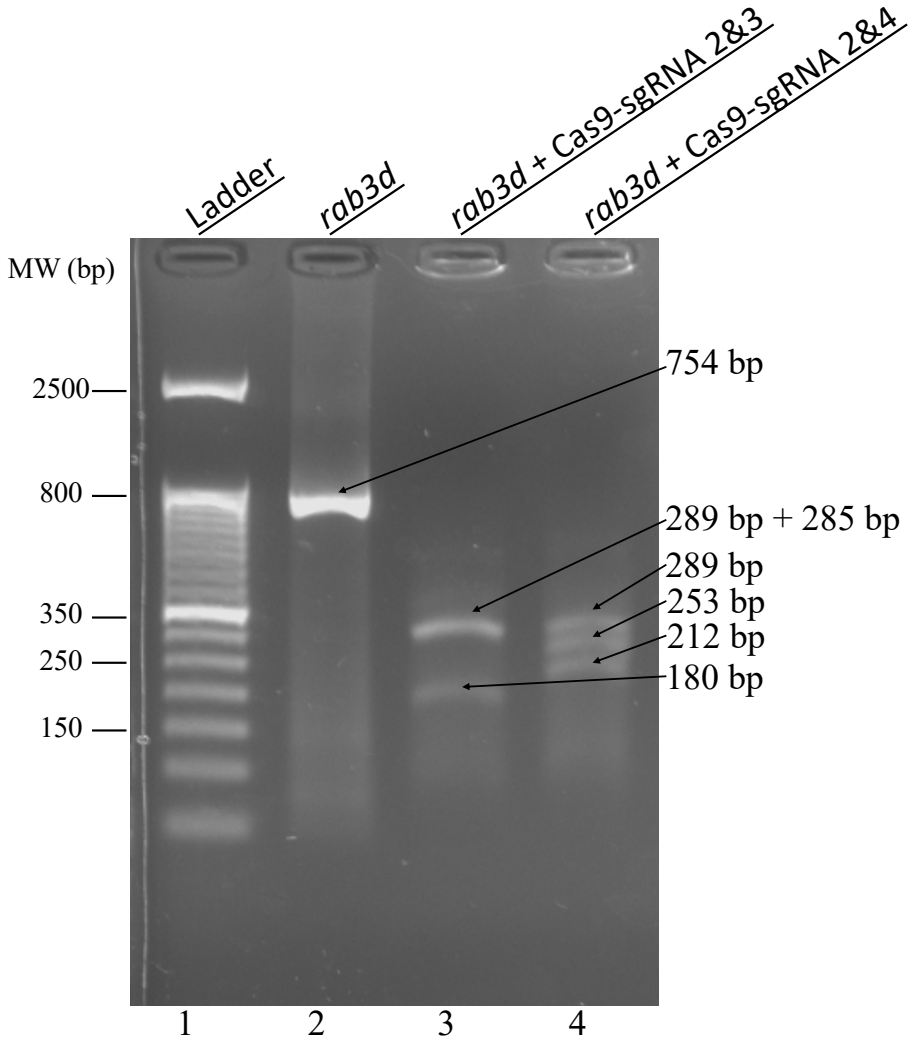

Fig. 6: sgRNA(2-4)-CRISPR-Cas9 *in vitro* **Screen upon *rab3d* Amplicon:** 1: Ladder, 2: *rab3d* amplicon, 3: *rab3d* amplicon cut by Cas9-sgRNA 2&3, 4: *rab3d* amplicon cut by sgRNA 2&4. Molecular weights labeled to the right are those expected of the products.

IV. Discussion

The sgRNAs targeting exon 1 of *rab3d* within the *X. maculatus* JP 163 A genome were designed and tested *in vitro* with *rab3d* amplicon cleavage successfully. The *in vitro* knockout of *rab3d* from the *X. maculatus* genome concludes the first step in creating *X. maculatus* knockouts in a vertebrate animal model who naturally has the potential to develop malignant melanoma. We recently discovered that *rab3d* is the oncogenic inhibiting factor preventing the spontaneous presentation of lethal melanoma in *Xiphophorus* within the GKA model [8]. Therefore, future directions of this project remain in completing the *in vivo rab3d* knockouts in *X. maculatus* JP163 A animals utilizing the identified sgRNA's in this study. We expect to see spontaneous melanomagenesis within *rab3d* knockout *X. maculatus* animals.

REFERENCES

1 Schartl, M. Beyond the zebrafish: diverse fish species for modeling human disease. *Dis Model Mech* **7**, 181-192, doi:10.1242/dmm.012245 (2014).

2 Walter, R. B. & Kazianis, S. Xiphophorus interspecies hybrids as genetic models of induced neoplasia. *ILAR J* **42**, 299-321 (2001).

3 Gordon, M. Hereditary Basis of Melanosis in Hybrid Fishes. *The American Journal of Cancer* **15**, 1495-1523, doi:10.1158/ajc.1931.1495 (1931).

4 Adam, D., Dimitrijevic, N. & Schartl, M. Tumor suppression in Xiphophorus by an accidentally acquired promoter. *Science* **259**, 816-819, doi:10.1126/science.8430335 (1993).

5 Wittbrodt, J. *et al.* Novel putative receptor tyrosine kinase encoded by the melanoma-inducing Tu locus in Xiphophorus. *Nature* **341**, 415-421, doi:10.1038/341415a0 (1989).

6 Patton, E. E., Mathers, M. E. & Schartl, M. Generating and analyzing fish models of melanoma. *Methods Cell Biol* **105**, 339-366, doi:10.1016/B978-0-12-381320-6.00014-X (2011).

7 Schartl, M. & Walter, R. B. Xiphophorus and Medaka Cancer Models. *Adv Exp Med Biol* **916**, 531-552, doi:10.1007/978-3-319-30654-4_23 (2016).

8 Lu, Y. *et al.* Oncogenic allelic interaction in Xiphophorus highlights hybrid incompatibility. *Proc Natl Acad Sci U S A*, doi:10.1073/pnas.2010133117 (2020).

9 Costin, G. E. & Hearing, V. J. Human skin pigmentation: melanocytes modulate skin color in response to stress. *FASEB J* **21**, 976-994, doi:10.1096/fj.06-6649rev (2007).

10 Cooper, C. D. & Raible, D. W. Mechanisms for reaching the differentiated state: Insights from neural crest-derived melanocytes. *Semin Cell Dev Biol* **20**, 105-110, doi:10.1016/j.semcdb.2008.09.008 (2009).

11 Le Guellec, D., Morvan-Dubois, G. & Sire, J. Y. Skin development in bony fish with particular emphasis on collagen deposition in the dermis of the zebrafish (Danio rerio). *Int J Dev Biol* **48**, 217-231, doi:10.1387/ijdb.15272388 (2004).

12 Shain, A. H. & Bastian, B. C. From melanocytes to melanomas. *Nat Rev Cancer* **16**, 345-358, doi:10.1038/nrc.2016.37 (2016).

13 Guy, G. P., Jr. *et al.* Vital signs: melanoma incidence and mortality trends and projections - United States, 1982-2030. *MMWR Morb Mortal Wkly Rep* **64**, 591-596 (2015).

14 Rigel, D. S. & Carucci, J. A. Malignant melanoma: prevention, early detection, and treatment in the 21st century. *CA Cancer J Clin* **50**, 215-236; quiz 237-240, doi:10.3322/canjclin.50.4.215 (2000).

15 Miller, R. *et al.* Epidemiology and survival outcomes in stages II and III cutaneous melanoma: a systematic review. *Melanoma Manag* **7**, MMT39, doi:10.2217/mmt-2019-0022 (2020).

16 Ferlay, J. *et al.* Estimating the global cancer incidence and mortality in 2018: GLOBOCAN sources and methods. *Int J Cancer* **144**, 1941-1953, doi:10.1002/ijc.31937 (2019).

17 Domingues, B., Lopes, J. M., Soares, P. & Populo, H. Melanoma treatment in review. *Immunotargets Ther* **7**, 35-49, doi:10.2147/ITT.S134842 (2018).

18 Ercolano, G. *et al.* Knockdown of PTGS2 by CRISPR/CAS9 System Designates a New Potential Gene Target for Melanoma Treatment. *Front Pharmacol* **10**, 1456, doi:10.3389/fphar.2019.01456 (2019).

19 Chapman, P. B. *et al.* Improved survival with vemurafenib in melanoma with BRAF V600E mutation. *N Engl J Med* **364**, 2507-2516, doi:10.1056/NEJMoa1103782 (2011).

20 Schadendorf, D. *et al.* Pooled Analysis of Long-Term Survival Data From Phase II and Phase III Trials of Ipilimumab in Unresectable or Metastatic Melanoma. *J Clin Oncol* **33**, 1889-1894, doi:10.1200/jco.2014.56.2736 (2015).

21 McDermott, J. & Jimeno, A. Pembrolizumab: PD-1 inhibition as a therapeutic strategy in cancer. *Drugs Today (Barc)* **51**, 7-20, doi:10.1358/dot.2015.51.1.2250387 (2015).

22 Schachter, J. *et al.* Pembrolizumab versus ipilimumab for advanced melanoma: final overall survival results of a multicentre, randomised, open-label phase 3 study (KEYNOTE-006). *Lancet* **390**, 1853-1862, doi:10.1016/s0140-6736(17)31601-x (2017).

23 Bhatia, S., Tykodi, S. S. & Thompson, J. A. Treatment of metastatic melanoma: an overview. *Oncology (Williston Park)* **23**, 488-496 (2009).

24 Winder, M. & Viros, A. Mechanisms of Drug Resistance in Melanoma. *Handb Exp Pharmacol* **249**, 91-108, doi:10.1007/164_2017_17 (2018).

25 Kozar, I., Margue, C., Rothengatter, S., Haan, C. & Kreis, S. Many ways to resistance: How melanoma cells evade targeted therapies. *Biochim Biophys Acta Rev Cancer* **1871**, 313-322, doi:10.1016/j.bbcan.2019.02.002 (2019).

26 Sarkisian, S. & Davar, D. MEK inhibitors for the treatment of NRAS mutant melanoma. *Drug Des Devel Ther* **12**, 2553-2565, doi:10.2147/DDDT.S131721 (2018).

27 Menezes, M. E. *et al.* Prospects of Gene Therapy to Treat Melanoma. *Adv Cancer Res* **138**, 213-237, doi:10.1016/bs.acr.2018.02.007 (2018).

28 Doudna, J. A. & Charpentier, E. Genome editing. The new frontier of genome engineering with CRISPR-Cas9. *Science* **346**, 1258096, doi:10.1126/science.1258096 (2014).

29 Jinek, M. *et al.* A Programmable Dual-RNA–Guided DNA Endonuclease in Adaptive Bacterial Immunity. *Science* **337**, 816-821, doi:10.1126/science.1225829 (2012).

30 Ran, F. A. *et al.* Genome engineering using the CRISPR-Cas9 system. *Nature Protocols* **8**, 2281-2308, doi:10.1038/nprot.2013.143 (2013).

31 Mali, P. *et al.* RNA-Guided Human Genome Engineering via Cas9. *Science* **339**, 823-826, doi:10.1126/science.1232033 (2013).

32 Gasiunas, G., Barrangou, R., Horvath, P. & Siksnys, V. Cas9–crRNA ribonucleoprotein complex mediates specific DNA cleavage for adaptive immunity in bacteria. *Proceedings of the National Academy of Sciences* **109**, E2579-E2586, doi:10.1073/pnas.1208507109 (2012).

33 Baylis, F. & McLeod, M. First-in-human Phase 1 CRISPR Gene Editing Cancer Trials: Are We Ready? *Curr Gene Ther* **17**, 309-319, doi:10.2174/1566523217666171121165935 (2017).

34 Rapoport, A. P. *et al.* NY-ESO-1–specific TCR–engineered T cells mediate sustained antigen-specific antitumor effects in myeloma. *Nature Medicine* **21**, 914-921, doi:10.1038/nm.3910 (2015).

35 Stadtmauer, E. A. *et al.* CRISPR-engineered T cells in patients with refractory cancer. *Science* **367**, doi:10.1126/science.aba7365 (2020).

36 Platt, Randall J. *et al.* CRISPR-Cas9 Knockin Mice for Genome Editing and Cancer Modeling. *Cell* **159**, 440-455, doi:https://doi.org/10.1016/j.cell.2014.09.014 (2014).

37 Sánchez-Rivera, F. J. & Jacks, T. Applications of the CRISPR–Cas9 system in cancer biology. *Nature reviews cancer* **15**, 387-395 (2015).

38 Stenmark, H. Rab GTPases as coordinators of vesicle traffic. *Nat Rev Mol Cell Biol* **10**, 513-525, doi:10.1038/nrm2728 (2009).

39 Kim, J. K. *et al.* Rab3a promotes brain tumor initiation and progression. *Mol Biol Rep* **41**, 5903-5911, doi:10.1007/s11033-014-3465-2 (2014).

40 Yang, J. *et al.* High expression of small GTPase Rab3D promotes cancer progression and metastasis. *Oncotarget* **6**, 11125-11138, doi:10.18632/oncotarget.3575 (2015).

41 Tan, P. Y. *et al.* Integration of regulatory networks by NKX3-1 promotes androgen-dependent prostate cancer survival. *Mol Cell Biol* **32**, 399-414, doi:10.1128/MCB.05958-11 (2012).

42 Chang, Y. C. *et al.* Secretory RAB GTPase 3C modulates IL6-STAT3 pathway to promote colon cancer metastasis and is associated with poor prognosis. *Mol Cancer* **16**, 135, doi:10.1186/s12943-017-0687-7 (2017).

43 Qiu, X., Valentijn, J. A. & Jamieson, J. D. Carboxyl-methylation of Rab3D in the rat pancreatic acinar tumor cell line AR42J. *Biochem Biophys Res Commun* **285**, 708-714, doi:10.1006/bbrc.2001.5224 (2001).

44 Luo, Y. *et al.* High expression of Rab3D predicts poor prognosis and associates with tumor progression in colorectal cancer. *Int J Biochem Cell Biol* **75**, 53-62, doi:10.1016/j.biocel.2016.03.017 (2016).

45 Altschul, S. F., Gish, W., Miller, W., Myers, E. W. & Lipman, D. J. Basic local alignment search tool. *J Mol Biol* **215**, 403-410, doi:10.1016/S0022-2836(05)80360-2 (1990).

46 Chen, X. *et al.* Dual sgRNA-directed gene knockout using CRISPR/Cas9 technology in Caenorhabditis elegans. *Scientific Reports* **4**, 7581, doi:10.1038/srep07581 (2014).

47 Bassett, A. R., Tibbit, C., Ponting, C. P. & Liu, J. L. Highly efficient targeted mutagenesis of Drosophila with the CRISPR/Cas9 system. *Cell Rep* **4**, 220-228, doi:10.1016/j.celrep.2013.06.020 (2013).

48 Wang, T., Wei, J. J., Sabatini, D. M. & Lander, E. S. Genetic screens in human cells using the CRISPR-Cas9 system. *Science* **343**, 80-84, doi:10.1126/science.1246981 (2014).

49 Chen, C., Fenk, L. A. & de Bono, M. Efficient genome editing in Caenorhabditis elegans by CRISPR-targeted homologous recombination. *Nucleic Acids Res* **41**, e193, doi:10.1093/nar/gkt805 (2013).